Molecular basis for increased susceptibility of Indigenous North Americans to seropositive rheumatoid arthritis

Stephen W. Scally[1*], Soi-Cheng Law[2*], Yi Tian Ting[1], Jurgen van Heemst[3], Jeremy Sokolove[4], Aaron J. Deutsch[5], E. Bridie Clemens[6], Antonis K. Moustakas[7], George K. Papadopoulos[8], Diane van der Woude[3], Irene Smolik[9], Carol A. Hitchon[9], David B. Robinson[9], Elizabeth D. Ferucci[10], Charles N. Bernstein[9], Xiaobo Meng[9], Vidyanand Anaparti[9], Tom Huizinga[3], Katherine Kedzierska[6], Hugh H. Reid[1], Soumya Raychaudhuri[11,12,13,14], René E. Toes[3#], Jamie Rossjohn[1,15,16#], Hani El-Gabalawy[9#]& Ranjeny Thomas[2#].

1. Infection and Immunity Program and The Department of Biochemistry and Molecular Biology, Biomedicine Discovery Institute Monash University, Clayton, Victoria 3800, Australia.

2. The University of Queensland Diamantina Institute, Translational Research Institute, Princess Alexandra Hospital, Brisbane, 4102, Australia.

3. Department of Rheumatology, Leiden University Medical Center, 2300 RC Leiden, The Netherlands.

4. Stanford University, Stanford, California, and VA Palo Alto Health Care System, Palo Alto, California.

5. Division of Genetics, Brigham and Women's Hospital, Harvard Medical School, Boston, Massachusetts, USA.

6. Department of Microbiology and Immunology, The University of Melbourne, at the Peter Doherty Institute for Infection and Immunity, Melbourne 3000, Victoria, Australia.

7. Faculty of Agricultural Technology, Technological Educational Institute of Ioanian Islands, Argostoli, Cephallonia, Greece.

8. Laboratory of Biochemistry and Biophysics, Faculty of Agricultural Technology, Epirus Institute of Technology, Arta, Greece.

9. Arthritis Centre, University of Manitoba, Winnipeg, Manitoba, Canada.

10. Division of Community Health Services, Alaska Native Tribal Health Consortium, Anchorage, Alaska, USA.

11. Department of Medicine, Brigham and Women's Hospital and Harvard Medical School, Boston, USA.

12. Program in Medical and Population Genetics, Broad Institute of MIT and Harvard, Cambridge, USA.

13. Partners Center for Personalized Genetic Medicine, Boston, USA

14. Arthritis Research UK Centre for Genetics and Genomics, University of Manchester, Manchester, UK.

15. Institute of Infection and Immunity, Cardiff University School of Medicine, Heath Park, Cardiff CF14 4XN, UK.

16. Australian Research Council Centre of Excellence in Advanced Molecular Imaging, Monash University, Clayton, Victoria 3800, Australia.

*Stephen W. Scally and Soi-Cheng Law contributed equally to this work.

#René E. Toes (R.E.M.Toes@lumc.nl), Jamie Rossjohn (jamie rossjohn jamie.rossjohn@monash.edu), Hani El-Gabalawy (Hani El-Gabalawy Hani.Elgabalawy@umanitoba.ca) and Ranjeny Thomas (Ranjeny.thomas@uq.edu.au) are co-senior and co-corresponding authors.

Abstract

Objective: The pathogenetic mechanisms by which *HLA-DRB1* alleles are associated with ACPA-positive rheumatoid arthritis (RA) are incompletely understood. RA high-risk *HLA-DRB1* alleles are known to share a common motif, the "shared susceptibility epitope (SE)". Here, the electro-positive P4-pocket of HLA-DRB1 accommodates self-peptide residues containing citrulline but not arginine. HLA-DRB1 His/Phe13β stratifies with ACPA-positive RA, while His13βSer polymorphisms stratify with ACPA-negative RA and RA-protection. Indigenous North American (INA) populations have high risk of early-onset ACPA-positive RA, whereby HLA-DRB1*04:04 and 14:02 are implicated as risk factors for RA in INA. However, HLA-DRB1*14:02 has a His13βSer polymorphism. Therefore, we aimed to verify this association and determine its molecular mechanism.

Methods: HLA genotype was compared in 344 INA RA patients and 352 controls. Structures of HLA-DRB1*1402-class II loaded with vimentin-64Arg$_{59-71}$, vimentin-64Cit$_{59-71}$ and fibrinogenβ-74Cit$_{69-81}$ were solved using X-ray crystallography. Vimentin-64Cit$_{59-71}$ and vimentin$_{59-71}$-specific CD4+ T cells were characterised by flow cytometry using pHLA tetramers. After sorting of antigen-specific T cells, TCRα and β chains were analyzed using multiplex, nested PCR and sequencing.

Results: ACPA^{+} RA in INA was independently associated with *HLA-DRB1*14:02*. Consequent to the His13βSer polymorphism and altered P4-pocket of HLA-DRB1*14:02, both citrulline and arginine were accommodated in opposite orientations. Oligoclonal autoreactive CD4+ effector T-cells reactive with both citrulline and arginine forms of vimentin$_{59-71}$ were observed in HLA-DRB1*14:02^{+} RA patients and at-risk ACPA^{-} first-degree relatives. HLA-DRB1*14:02-vimentin$_{59-71}$-specific and HLA-DRB1*14:02-vimentin-64Cit$_{59-71}$-specific CD4+ memory T cells were phenotypically distinct populations.

Conclusion: HLA-DRB1*14:02 broadens the capacity for citrullinated and native self-peptide presentation and T cell expansion, increasing risk of ACPA+ RA.

INTRODUCTION

Rheumatoid arthritis (RA) is an autoimmune disease with peak incidence in the sixth decade and prevalence of 1% in Caucasians, linked to *HLA-DRB1*. *HLA-DRB1* alleles associated with anti-citrullinated peptide antibody (ACPA)-positive RA in Caucasians share a common motif in the third hypervariable region, the "shared susceptibility epitope (SE)" that was shown to accommodate citrullinated self-epitopes [1-3]. Citrulline is post-translationally modified from arginine during inflammation, ER stress and autophagy [4, 5]. Various RA-associated citrullinated (Cit) autoantigens, recognised by ACPA, are present in inflamed lung and joint tissues. Low titre ACPA develop in healthy individuals associated with environmental risk factors including smoking, bronchiectasis and periodontitis, but are unrelated to *HLA-DR SE* [6-11]. In the immediate pre-RA period, ACPA isotype diversity and titre increase – a process associated with antigen-specific CD4+ T cell help for affinity maturation in germinal centres [8]. *HLA-DR SE* are associated with ACPA+ RA rather than ACPA, implying that presentation of Cit-autoantigens bound to HLA-DR SE molecules to CD4+ T cells is associated with RA development in at-risk individuals carrying *HLA-DR SE*.

Based on genome-wide studies (GWAS) in patients of predominantly Caucasian and Asian ethnicity, *HLA* alleles associated with ACPA-positive RA, including *HLA-DRB1*04:01, *04:05* and **01:01* (odds ratios of 2.17-4.44) were found to share a common motif at amino acid positions 11, 13, 71 and 74, influencing the P4 antigen-binding pocket of DRβ [2]. Moreover, Val11βSer and His13βSer polymorphisms within that motif were found in genomic studies to stratify with ACPA-negative RA in Caucasians [3]. The discovery that P4-Cit was

accommodated, but the positively-charged Arg was excluded from the electro-positive P4-pocket of HLA-DRB1*04:01/04 suggested that preferential presentation of Cit-autoantigens might underpin the association of $ACPA^+$ RA with the SE [12]. While HLA-DRB1*04:01-restricted $CD4^+$ memory T cells recognizing Cit-autoantigens have been reported in RA patients [12, 13], their role in disease development is unclear. To date it has not been determined how autoreactive T cells respond to citrullinated autoantigen in RA and whether they undergo clonal expansion due to antigen experience in RA patients or in HLA-SE+ at-risk first-degree relatives (FDR).

Furthermore, in unravelling antigen presentation by HLA-DR molecules in RA, the ethnic mix of the samples included in GWAS may skew interpretations of amino acids contributing to binding motifs made from genomic studies. The Indigenous North American (INA) population has a 2-3 fold higher prevalence of RA than Caucasians, with RA onset peaking earlier, in the fourth decade of life [14]. Moreover, 90% of INA RA patients are $ACPA^+$. In this population, FDR have a high prevalence of joint symptoms and of ACPA positivity, predisposing them to RA [15, 16]. To date, the *HLA* association with RA in INA has been sought in studies of <100 patients [17-19]. These studies suggested that the *HLA-SE*-alleles also predispose to RA in INA. *HLA-DRB1*04:04* is the most frequent *SE*-allele in these populations followed by *HLA-DRB1*14:02*. Since HLA-DRB1*14:02 carries the β13Ser residue, which was interpreted to stratify with ACPA-negative RA [3], we investigated the genetic and underlying molecular bases for the increased risk of severe $ACPA^+$ RA in INA.

MATERIALS AND METHODS

Study participants

RA cases, non-RA controls and first-degree relatives (FDR) were recruited from INA populations in Central Canada (Cree, Ojibway, and Ojicree) and Alaska Native people (from Southcentral and Southeast Alaska). DNA for HLA typing, serum and PBMC were isolated.

*HLA-DRB1*14:02 expression and purification*

Peptide-loaded HLA-DRB1*14:02 molecules were purified, crystallised and structures determined.

Multiplex ACPA assay

Serum levels of antibodies targeting 40 putative RA-associated autoantigens were measured using a custom bead-based immunoassay on a Bio-Plex platform, as previously described [20].

Tetramer staining and analysis of TCR repertoire

Tetramer staining and TCR repertoire analysis used previously published methods, with some modifications [12, 21, 22].

Details of all methods available in **Supplementary methods**, **Supplementary Table 1** and **Supplementary Figure 1**.

RESULTS

*HLA-DRB1*14:02* is independently associated with ACPA$^+$ RA in INA

Although very rare in Caucasians and Asians, *HLA-DRB1*14:02* has a prevalence of up to 80% in some INA populations, suggesting a particular survival advantage against pathogens [17-19]. To determine the *HLA-DRB1* association with ACPA$^+$ RA in INA, we genotyped the largest cohort available, comprising 344 INA RA patients and 352 controls. Rheumatoid factor (RF) and ACPA status was known in 241/344 RA patients: 90% were seropositive (RF and/or ACPA$^+$). In seropositive RA patients, 32% carried *HLA-DRB1*14:02* and 45% *HLA-*

*DRB1*04:04*. One third of patients carrying *HLA-DRB1*14:02* carried an additional *SE* allele. In healthy controls, 28% carried *DRB1*14:02*, 22% *HLA-DRB1*04:04* and 17% carried an additional *SE* allele. After stratifying RA patients according to HLA-status, *HLA-DRB1*14:02* was a risk factor for seropositive RA (OR 2.38) independent of other *SE* alleles (**Table 1**). In INA RA patients, the most commonly associated other *SE* allele is *HLA-DRB1*04:04* (**Table 1**). In INA, RA risk was associated with *HLA-DRB1* alleles with a conserved SE motif at 71 and 74 in all RA (OR = 2.48, 95% CI = 1.70-3.60, P<0.0001) and in seropositive RA (OR = 2.46, 95% CI = 1.58-3.81, P=0.0001) patients (**Table 1**). We note that without genome-wide genotyping, we cannot rule out the possibility of confounding due to case-control differences in ancestry.

To stratify ACPA response with genotype, sera of 232 INA RA patients were tested in a multiplex ACPA antigen array and given an ACPA score (sum of all normalized ACPA titers divided by number of epitopes) [23]. ACPA score was higher in INA RA patients who were either *HLA-DRB1*14:02* homozygotes or *HLA-DRB1*14:02/HLA-SE* compound heterozygotes than those who were *HLA-SE*-negative ($p<0.05$). ACPA scores in *HLA-DRB1*14:02*$^+$ patients were equivalent to those in *HLA-SE*$^+$ patients lacking *HLA-DRB1*14:02*. ACPA specificities increased among *HLA-DRB1*14:02*$^+$ patients included vimentin-64Cit$_{58\text{-}77}$, filaggrin-56Cit$_{48\text{-}65}$ and fibrinogen-α-573Cit$_{556\text{-}575}$ (**Figure 1a, 1b**). Thus, despite polymorphisms of Val11βSer and His13βSer, INA individuals carrying *HLA-DRB1*14:02* develop a broad ACPA-response whether or not they carry other *SE* alleles. This implies binding and presentation of a variety of Cit-autoantigens by *HLA-DRB1*14:02* to autoreactive T cells.

Accommodation of arginine and citrulline residues within the P4 pocket of HLA-DRB1*14:02.

The HLA-DRB1 chain contains 12 polymorphic residues that have been directly implicated in peptide binding [24]. HLA-DRB1*14:02 differs from *04:01, *04:04 or *01:01 in 8 of these residues, which shape P4, P6, P7 and P9 pockets (**Figure 2a**). To test whether HLA-DRB1*14:02 presents autoantigens differently to HLA-DRB1*04:01, *04:04 or *01:01, we compared the capacity of each HLA binding pocket to accommodate Cit and Arg residues using the influenza-derived $HA_{305-319}$ peptide [25-28]. Conversion of Arg to Cit at peptide-positions interacting with P4 enhanced peptide binding affinity to HLA-DRB1*01:01 by 2 fold and to *04:01 by 10 fold. Conversion of Arg to Cit at peptide-positions interacting with the P6 and P9 pockets enhanced peptide binding affinity to HLA-DRB1*01:01, and P7 to HLA-DRB1*04:01. In contrast, peptides containing an Arg or Cit residue at positions interacting with P4 of HLA-DRB1*14:02 had similar binding affinity, and peptides containing Arg at positions interacting with P6 and P9 had increased affinity relative to Cit-peptides (**Figure 2b**). While the IC50 of the self-peptide, vimentin64Cit_{59-71}, was decreased by 1.3 fold relative to the 64-Arg variant for HLA-DRB1*01:01, and the 64-Arg variant did not bind *04:01, HLA-DRB1*14:02 bound both 64-Arg and 64-Cit variants with IC50 of 19 μM (**Figure 2c**), indicating that both residues could be accommodated within P4 of HLA-DRB1*14:02, or that HLA-DRB1*14:02 presented in differing peptide binding registers.

Structural basis of peptide presentation by HLA-DRB1*14:02

We solved the structure of HLA-DRB1*14:02 in complex with vimentin64Arg_{59-71}, vimentin64Cit_{59-71} and fibrinogenβ74Cit_{69-81} (**Supplementary Table 2**, **Figures 3a-d**). These HLA-DRB1*14:02 structures overlaid closely (**Figure 3e**), ruling out markedly differing binding modes to accommodate these differing epitopes. Within the HLA-DRB1*14:02-vimentin64Cit_{59-71} and HLA-DRB1*14:02-vimentin64Arg_{59-71} structures, Tyr, Ser and Arg occupied the P1, P6 and P9 pockets of HLA-DRB1*14:02, respectively (**Figure 3b,c**). In the HLA-DRB1*14:02- fibrinogen β74Cit_{69-81} complex, Tyr, Ala and Ala occupied the P1, P6 and

P9 pockets of HLA-DRB1*14:02, respectively (**Figure 3d**). The largest structural differences between the peptides in each binary complex centered on the residue occupying the P4-pocket of HLA-DRB1*14:02, namely P4-Cit and P4-Arg in vimentin64Cit$_{59-71}$, fibrinogen β74Cit$_{69-81}$ and vimentin64Arg$_{59-71}$, respectively. These structures clearly show that P4-Arg and P4-Cit are presented in alternative orientations, whereby the P4-Arg projects inwards, whereas the P4-Cit projects outwards from the HLA-DRB1*14:02 Ag-binding cleft (**Figures 3f-h**). The P4-Arg is buried in the pocket to avoid interactions with the positively charged β71Arg residue. This orientation is promoted by β11Ser and β13Ser, whereupon these two small polar residues allow the accommodation of Arg by providing the necessary space and H-bonding partners (**Figure 3f**). Larger residues in HLA-DRB1*04:01 (β11Val and β13His) and HLA-DRB1*01:01 (β11Leu and β13Phe) as well as the charge repulsion of β13His in HLA-DRB1*04:01 would prevent the accommodation of Arg at P4 [12]. The P4-Arg residue is stabilized by H-bonds with Ser11β, Ser13β and Tyr30β, and a salt bridge with Glu28β (**Figure 3f**). In contrast, the P4-Cit sits upright in both Cit-epitopes, similar to its orientation in P4-Cit from Cit epitopes presented by HLA-DRB1*04:01/04:04 (**Figures 3g,h**) [12]. The P4-Cit is stabilized by H-bonds with Arg71β and Gln70β (**Figure 3g,h**). Accordingly, we demonstrate a conserved positioning of the citrulline residue in two distinct epitopes that contrast the orientation of the non-citrullinated residue within the P4-pocket. Similar to its orientation in HLA-DRB1*04:01 and HLA-DRB1*04:04 [12, 29], P4-Cit was solvent-exposed in HLA-DRB1*14:02, and could potentially interact with TCR.

Antigen-experienced, oligoclonally-expanded T cells recognize Arg and Cit-variants of vimentin$_{59-71}$ presented by HLA-DRB1*14:02

Although both vimentin 64-Arg and 64-Cit variant peptides bound HLA-DRB1*14:02, only P4-Cit sits upright, and thereby potentially able to interact with the TCR. Thus, we addressed whether autoreactive T cells with TCRs recognizing one or both epitopes were present in the

periphery and displayed evidence of in vivo expansion in response to antigen presentation. We analysed T cells recognizing HLA-DRB1*14:02-vimentin64Cit$_{59\text{-}71}$ and HLA-DRB1*1402-vimentin$_{59\text{-}71}$ tetramers in ten HLA-DRB1*14:02^{+} INA RA patients, ten HLA-DRB1*14:02^{+} ACPA^{-} FDR, and 6 HLA-DRB1*14:02^{+} non-INA healthy control (HC) subjects. FDR in the INA population have a high burden of environmental risk factors for RA, a high level of background HLA-DR SE genes, high inflammatory CRP and a high prevalence of joint symptoms [16]. Among the 13 FDR studied (**Supplementary Table 3**) 85% were past smokers and 31% had an abnormal CRP >8. Therefore we could compare T cells recognizing vimentin or Cit-vimentin in individuals both with RA and with high risk of future RA. Similar frequencies of CD4^{+} T cells recognized vimentin 64-Arg and 64-Cit variant peptides in HLA-DRB1*14:02^{+} FDR and RA patients, and with similar tetramer staining intensity (MFI) (**Figure 4a, b**). In all individuals, HLA-DRB1*14:02-vimentin64Cit$_{59\text{-}71}$-reactive and HLA-DRB1*14:02-vimentin$_{59\text{-}71}$-reactive CD4^{+} T cells were significantly enriched in CD25^{+}CD127^{+} effector (Teff) and CD25^{+}CD127^{-} regulatory T cells (Treg) [30] compared to the total CD4^{+} PB T cell pool (Treg $p<0.0001$, Teff $p<0.05$, **Figure 4c**), consistent with antigen experience in vivo. This enrichment did not differ between RA patients and FDR, indicating that antigen experience and formation of memory develops before the onset of ACPA in INA. The numbers of circulating HLA-DRB1*14:02-vimentin64Cit$_{59\text{-}71}$-reactive and HLA-DRB1*14:02-vimentin$_{59\text{-}71}$-reactive CD4^{+} T cells were correlated in each individual RA patient and FDR ($r^2=0.74$, $p<0.0001$, **Figure 4d**).

T cell effector function is balanced by the suppressive activity of Treg [31]. The ratio of HLA-DRB1*14:02-vimentin$_{59\text{-}71}$Cit64-reactive and HLA-DRB1*14:02-vimentin$_{59\text{-}71}$-reactive Teff/ Treg was significantly lower than that of the total CD4^{+} T cell pool in RA patients and FDR ($p<0.001$, **Figure 4e**), consistent with active regulation of the autoreactive T cells. To understand the particular role of CD4^{+} T cells of each vimentin specificity further, we analysed

an additional 6 HLA-DRB1*14:02$^+$ INA individuals (3 with RA, 3 FDR, clinical details in **Supplementary Table 3**) and 6 HLA-DRB1*14:02$^+$ HC for markers of memory T cell activation and differentiation relative to total CD4+ T cells. In INA RA patients and FDR the proportion of CD28$^+$ memory T cells was significantly higher among vimentin$_{59\text{-}71}$-reactive CD4$^+$ T cells ($p<0.05$, **Figure 4f**). Moreover, cells expressing CD69 were significantly enriched among vimentin$_{59\text{-}71}$-reactive CD4$^+$ T cells in these individuals. Some CD69$^+$ vimentin$_{59\text{-}71}$-reactive memory CD4$^+$ T cells also expressed NKG2D (**Figure 4g**). In contrast, HC Vimentin64Cit$_{59\text{-}71}$-reactive and vimentin$_{59\text{-}71}$-reactive CD4$^+$ T cells did not differ in phenotype from total CD4$^+$ T cells and the numbers of vimentin64Cit$_{59\text{-}71}$-reactive and vimentin$_{59\text{-}71}$-reactive CD4$^+$ T cells did not correlate (**Supplementary Figure 2**). Thus, in INA FDR and RA patients but not HC, T cells reflect antigen-driven activation and differentiation.

TCR bias and oligoclonal TCR reactive with vimentin64Cit$_{59\text{-}71}$ and vimentin$_{59\text{-}71}$

To obtain evidence of in vivo expansion in HLA-DRB1*14:02$^+$ INA, we used multiplex PCR to sequence the TCRs from a total of 53 single vimentin$_{59\text{-}71}$-reactive and 71 vimentin-64Cit$_{59\text{-}71}$-reactive tetramer-positive CD4$^+$ T cells derived from five HLA-DRB1*14:02$^+$ RA patients and five HLA-DRB1*14:02$^+$ FDR. *TRAV* and *TRBV* gene usage among CD4$^+$ T cells reactive to each vimentin epitope was generally diverse in RA and FDR (**Supplementary Table 4**). However, *TRBV20-1* and *TRBV30* were preferentially used variable gene segments for recognition of vimentin 64-Arg and 64-Cit variant peptides bound to HLA-DRB1*14:02 (**Figure 4h**). *TRAV13-2* and *TRAV26-1* were preferentially used variable gene segments among both vimentin$_{59\text{-}71}$- reactive and vimentin-64Cit$_{59\text{-}71}$- reactive TCRs. Use of preferential variable gene segments in the repertoires of T cells recognizing each epitope was observed in both RA patients and FDR and suggested underlying oligoclonality of the autoreactive T cell populations when compared with the total CD3$^+$ T cell population (**Figure 4h**). Indeed, multiple vimentin64Cit$_{59\text{-}71}$- reactive and vimentin$_{59\text{-}71}$- reactive CD4$^+$ T cells bearing the same

CDR3α and/or CDR3β sequences were identified amongst the single cells sorted from 2 of the RA patients and 2 FDR (**Table 2**). In two FDR, $CD4^+$ T cells bearing the same TRBV30 CDR3 sequences were identified multiple times among single cells reactive for vimentin 64-Arg and 64-Cit variant peptides bound to HLA-DRB1*14:02. In one RA patient, the same TRBV2 CDR3 sequences were identified multiple times among single vimentin-64Cit$_{59\text{-}71}$-reactive $CD4^+$ T cells, and in another patient, the same TRBV10-3 CDR3 sequences were identified multiple times among single vimentin$_{59\text{-}71}$-reactive $CD4^+$ T cells. These repeated CDR3α and CDR3β sequences indicate antigen-reactive clonal expansion within the blood of these HLA-DRB1*14:02$^+$ patients and at-risk FDR (**Table 2**). In all cases, clonally expanded tetramer$^+$ T cells were $CD4^+CD25^+CD127^+$ Teff, as determined by index sorting. Individuals in whom any oligoclonal sequences were detected in PB were more likely to be *HLA-DRB1*14:02* homozygous or *HLA-DRB1*14:02/*04:04* compound heterozygous than individuals without oligoclonal expansion ($p<0.05$, Chi^2 test). Remarkably, a common TRBV30 CDR3 sequence (SI/VGAGNQPQ) was expanded in the blood of 2 individual FDR, which in each case encoded TCRs recognizing vimentin$_{59\text{-}71}$ as well as vimentin-64Cit$_{59\text{-}71}$. Of 34 sorted antigen-reactive T cells yielding productive TRBV gene sequences from FDR, 23.5% contained this CDR3β sequence. We used retroviral vectors encoding HLA-DR14:02-vimentin$_{59\text{-}71}$-restricted TCR P2F3 (**Supplementary Table 4, bold**) to transduce the αβ TCR-deficient SKW-3 cell line [32, 33]. When stimulated with HLA-DRB1*14:02-vimentin$_{59\text{-}71}$ or vimentin-64Cit$_{59\text{-}71}$ tetramers, P2F3 SKW-3 cells upregulated pERK relative to HLA-DRB1*14:02-CLIP tetramers (**Figure 4i**), confirming that TCR identified from cells with HLA-DRB1*14:02-vimentin$_{59\text{-}71}$ tetramer reactivity recognize vimentin$_{59\text{-}71}$ and vimentin-64Cit$_{59\text{-}71}$ in the context of HLA-DRB1*14:02.

The biased TCR usage suggests a structural requirement for conserved amino acid sequences to recognise vimentin$_{59\text{-}71}$ and vimentin-64Cit$_{59\text{-}71}$. Nucleotide sequences encoding TRBV30

CDR3 reveal that although the second N region at the D-J junction in each TCR is different, they encode the same amino acid sequence (**Table 2**). These data implicate convergent recombination events in the selection of this sequence during TCR gene rearrangement [34].

DISCUSSION

*HLA-DRB1*14:02* and *HLA-DRB1*04:04* are shown to be independent risk alleles for ACPA$^+$ RA in the INA population. Analysis of the structures and T cell responses to citrullinated and non-citrullinated epitopes shows that, consequent to the His13βSer polymorphism and altered P4-pocket, HLA-DRB1*14:02 can present both variant peptides. This contrasts with structures of HLA-DRB1*04:01 and *04:04, in which Cit but not Arg can be accommodated in P4 [12, 29]. Presentation of both 64-Cit and 64-Arg vimentin$_{59\text{-}71}$ variants promoted autoreactive CD4$^+$ T cell activation and differentiation to Teff and Treg, and clonal expansion of Teff in *HLA-DRB1*14:02*$^+$ RA patients and at-risk FDR. In *HLA-DRB1*14:02*+ HC, we observed no activation or differentiation of antigen-specific T cells above the background total CD4+ T cells. Previous studies of CD4+ T cells in individuals carrying Caucasian SE alleles show that T cell responses to Cit-autoantigenic peptides are increased relative to Arg-variant peptides [12, 29, 35, 36], reinforcing that T cell function aligns with HLA-DR-peptide structure.

We show preferential variable gene segments and clonally-expanded TCR among vimentin$_{59\text{-}71}$- and vimentin-64Cit$_{59\text{-}71}$–reactive CD4$^+$CD25$^+$CD127$^+$ Teff sorted from RA patients and FDR, including a public TRBV CDR3. These data suggest that presentation of vimentin self-epitopes in vivo continues in genetically predisposed individuals before and after onset of RA, and selects T cells making productive TCR rearrangements, as identified by the nucleotide sequences, for antigen recognition and T cell expansion.

Although limited by small sample numbers, the phenotypic profiles of 64-Cit and 64-Arg variant-specific autoreactive T cells appeared to be different. The fibroblast antigen, vimentin, has widespread tissue expression [37]. Vimentin 64-Arg-specific memory CD4+ T cells specifically expressed CD69. CD69 is a marker of recent activation or tissue residency and exposure to cytokines such as TNF [30], suggesting that vimentin$_{59\text{-}71}$-reactive T cells are activated in tissue inflammatory sites. NKG2D signifies Teff costimulatory function and is TNF-activated [31]. Intriguingly, our data suggest cross-reactivity of some TCRs for the 64-Cit and 64-Arg variants: cell frequency of each specificity was correlated, the public clonotype occurred in T cells reactive with each variant, and T cells expressing TCR P2F3 were activated with both tetramers. In general, co-expansion of T cells recognising Cit and Arg variants might be advantageous, e.g. for cross-protection against infectious antigens requiring rapid immunity [38-40]. This suggests a hypothesis for persistence of *HLA-DRB1*14:02* in the INA population, even though its molecular structure permits presentation of multiple self-antigens driving ACPA$^+$ RA.

Low titre ACPA develop in healthy individuals independent of HLA-DR SE, particularly in inflammatory contexts [6-8, 10, 11]. In HLA-DR SE$^+$ individuals, memory T cells driven by antigen experience would provide required B cell help for increased titres and epitope spreading in patients developing RA [8, 41, 42]. Since HLA-DRB1*14:02 broadens capacity for autoantigen presentation and T cell expansion, our study provides a mechanism for enhanced risk of early onset of ACPA+ RA in INA.

Acknowledgments

We thank the staff at the National Australian Synchrotron for assistance with data collection and staff at the Monash Macromolecular crystallization facility and Nishta Ramnoruth for assistance with flow cytometric staining. This work was supported by Australian National

Health and Medical Research Council (NHMRC), Australian Research Council (ARC) and Canadian Institutes of Health Research (CIHR: MOP77700) funding. J.R. is an ARC Australian Laureate Fellow and R.T. an NHMRC Fellow.

References

1 Gregersen PK, Silver J, Winchester RJ. The shared epitope hypothesis: an approach to understanding the molecular genetics of suseptibility to rheumatoid arthritis. Arthritis Rheum. 1987; **30**:1205-13.
2 Raychaudhuri S, Sandor C, Stahl EA, et al. Five amino acids in three HLA proteins explain most of the association between MHC and seropositive rheumatoid arthritis. Nat Genet. 2012; **44**:291-96.
3 Han B, Diogo D, Eyre S, et al. Fine mapping seronegative and seropositive rheumatoid arthritis to shared and distinct HLA alleles by adjusting for the effects of heterogeneity. Am J Hum Genet. 2014; **94**:522-32.
4 Ireland JM, Unanue ER. Autophagy in antigen-presenting cells results in presentation of citrullinated peptides to CD4 T cells. J Exp Med. 2011; **208**:2625-32.
5 Ireland JM, Unanue ER. Processing of proteins in autophagy vesicles of antigen-presenting cells generates citrullinated peptides recognized by the immune system. Autophagy. 2012; **8**:429-30.
6 Padyukov L, Silva C, Stolt P, et al. A gene-environment interaction between smoking and shared epitope genes in HLA-DR provides a high risk of seropositive rheumatoid arthritis. Arthritis Rheum. 2004; **50**:3085-92.
7 Quirke AM, Perry E, Cartwright A, et al. Bronchiectasis Is a Model for Chronic Bacterial Infection Inducing Autoimmunity in Rheumatoid Arthritis. Arthritis Rheumatol. 2015; **67**:2335-42.
8 Koning F, Thomas R, Rossjohn J, et al. Coeliac disease and rheumatoid arthritis: similar mechanisms, different antigens. Nat Rev Rheumatol. 2015; **11**:450-61.
9 Alpizar-Rodriguez D, Brulhart L, Mueller RB, et al. The prevalence of anticitrullinated protein antibodies increases with age in healthy individuals at risk for rheumatoid arthritis. Clin Rheumatol. 2017; **36**:677-82.
10 Fisher BA, Cartwright AJ, Quirke AM, et al. Smoking, Porphyromonas gingivalis and the immune response to citrullinated autoantigens before the clinical onset of rheumatoid arthritis in a Southern European nested case-control study. BMC Musculoskelet Disord. 2015; **16**:331.
11 Terao C, Asai K, Hashimoto M, et al. Significant association of periodontal disease with anti-citrullinated peptide antibody in a Japanese healthy population - The Nagahama study. J Autoimmun. 2015; **59**:85-90.
12 Scally SW, Petersen J, Law SC, et al. A molecular basis for the association of the HLA-DRB1 locus, citrullination, and rheumatoid arthritis. J Exp Med. 2013; **210**:2569-82.
13 James E, Rieck M, Pieper J, et al. Citrulline specific Th1 cells are increased in rheumatoid arthritis and their frequency is influenced by disease duration and therapy. Arthritis Rheumatol. 2014.
14 Peschken CA, Esdaile JM. Rheumatic diseases in North America's indigenous peoples. Semin Arthritis Rheum. 1999; **28**:368-91.
15 Ferucci ED, Darrah E, Smolik I, et al. Prevalence of anti-peptidylarginine deiminase type 4 antibodies in rheumatoid arthritis and unaffected first-degree relatives in indigenous North American Populations. J Rheumatol. 2013; **40**:1523-8.
16 Smolik I, Robinson DB, Bernstein CN, et al. First-degree relatives of patients with rheumatoid arthritis exhibit high prevalence of joint symptoms. J Rheumatol. 2013; **40**:818-24.

17 Willkens RF, Nepom GT, Marks CR, et al. Association of HLA-Dw16 with rheumatoid arthritis in Yakima Indians. Further evidence for the "shared epitope" hypothesis. Arthritis Rheum. 1991; **34**:43-7.
18 Nelson JL, Boyer G, Templin D, et al. HLA antigens in Tlingit Indians with rheumatoid arthritis. Tissue Antigens. 1992; **40**:57-63.
19 Williams RC, Jacobsson LT, Knowler WC, et al. Meta-analysis reveals association between most common class II haplotype in full-heritage Native Americans and rheumatoid arthritis. Hum Immunol. 1995; **42**:90-4.
20 Sokolove J, Bromberg R, Deane KD, et al. Autoantibody epitope spreading in the pre-clinical phase predicts progression to rheumatoid arthritis. PLoS One. 2012; **7**:e35296.
21 Tungatt K, Bianchi V, Crowther MD, et al. Antibody stabilization of peptide-MHC multimers reveals functional T cells bearing extremely low-affinity TCRs. J Immunol. 2015; **194**:463-74.
22 Wang GC, Dash P, McCullers JA, et al. T cell receptor alphabeta diversity inversely correlates with pathogen-specific antibody levels in human cytomegalovirus infection. Sci Transl Med. 2012; **4**:128ra42.
23 Wagner CA, Sokolove J, Lahey LJ, et al. Identification of anticitrullinated protein antibody reactivities in a subset of anti-CCP-negative rheumatoid arthritis: association with cigarette smoking and HLA-DRB1 'shared epitope' alleles. Ann Rheum Dis. 2015; **74**:579-86.
24 Geluk A, van Meijgaarden KE, Southwood S, et al. HLA-DR3 molecules can bind peptides carrying two alternative specific submotifs. J Immunol. 1994; **152**:5742-8.
25 Hennecke J, Wiley DC. Structure of a complex of the human alpha/beta T cell receptor (TCR) HA1.7, influenza hemagglutinin peptide, and major histocompatibility complex class II molecule, HLA-DR4 (DRA*0101 and DRB1*0401): insight into TCR cross-restriction and alloreactivity. J Exp Med. 2002; **195**:571-81.
26 Stern LJ, Brown JH, Jardetzky TS, et al. Crystal structure of the human class II MHC protein HLA-DR1 complexed with an influenza virus peptide. Nature. 1994; **368**:215-21.
27 James EA, Moustakas AK, Bui J, et al. HLA-DR1001 presents "altered-self" peptides derived from joint-associated proteins by accepting citrulline in three of its binding pockets. Arthritis Rheum. 2010; **62**:2909-18.
28 James EA, Moustakas AK, Bui J, et al. The binding of antigenic peptides to HLA-DR is influenced by interactions between pocket 6 and pocket 9. J Immunol. 2009; **183**:3249-58.
29 Gerstner C, Dubnovitsky A, Sandin C, et al. Functional and Structural Characterization of a Novel HLA-DRB1*04:01-Restricted alpha-Enolase T Cell Epitope in Rheumatoid Arthritis. Front Immunol. 2016; **7**:494.
30 Seddiki N, Santner-Nanan B, Martinson J, et al. Expression of interleukin (IL)-2 and IL-7 receptors discriminates between human regulatory and activated T cells. The Journal of Experimental Medicine. 2006; **203**:1693-700.
31 Sakaguchi S. Regulatory T cells: key controllers of immunologic self tolerance. Cell. 2000; **101**:455-58.
32 Gras S, Chen Z, Miles JJ, et al. Allelic polymorphism in the T cell receptor and its impact on immune responses. J Exp Med. 2010; **207**:1555-67.
33 Beringer DX, Kleijwegt FS, Wiede F, et al. T cell receptor reversed polarity recognition of a self-antigen major histocompatibility complex. Nat Immunol. 2015; **16**:1153-61.
34 Kedzierska K, Thomas PG, Venturi V, et al. Terminal deoxynucleotidyltransferase is required for the establishment of private virus-specific CD8+ TCR repertoires and facilitates optimal CTL responses. J Immunol. 2008; **181**:2556-62.
35 Law SC, Street S, Yu CH, et al. T-cell autoreactivity to citrullinated autoantigenic peptides in rheumatoid arthritis patients carrying HLA-DRB1 shared epitope alleles. Arthritis Res Ther. 2012; **14**:R118.

36 James EA, Rieck M, Pieper J, et al. Citrulline-specific Th1 cells are increased in rheumatoid arthritis and their frequency is influenced by disease duration and therapy. Arthritis Rheumatol. 2014; **66**:1712-22.
37 Kishaba Y, Matsubara D, Niki T. Heterogeneous expression of nestin in myofibroblasts of various human tissues. Pathol Int. 2010; **60**:378-85.
38 Furman D, Jojic V, Sharma S, et al. Cytomegalovirus infection enhances the immune response to influenza. Sci Transl Med. 2015; **7**:281ra43.
39 Chang MH, Moonesinghe R, Athar HM, et al. Trends in Disparity by Sex and Race/Ethnicity for the Leading Causes of Death in the United States-1999-2010. J Public Health Manag Pract. 2016; **22 Suppl 1**:S13-24.
40 Foote EM, Singleton RJ, Holman RC, et al. Lower respiratory tract infection hospitalizations among American Indian/Alaska Native children and the general United States child population. Int J Circumpolar Health. 2015; **74**:29256.
41 Hunt L, Hensor EM, Nam J, et al. T cell subsets: an immunological biomarker to predict progression to clinical arthritis in ACPA-positive individuals. Ann Rheum Dis. 2016; **75**:1884-9.
42 Janssen KM, Westra J, Chalan P, et al. Regulatory CD4+ T-Cell Subsets and Anti-Citrullinated Protein Antibody Repertoire: Potential Biomarkers for Arthritis Development in Seropositive Arthralgia Patients? PLoS One. 2016; **11**:e0162101.

Figures

Figure 1. HLA-DRB1*14:02 is associated with a broad ACPA response

Serum levels of antibodies targeting RA-associated Cit-autoantigens were measured in serum from 232 INA RA patients using a custom bead-based fluorescence immunoassay. Fluorescence intensities for 10 Cit-autoantigens and CCP were clustered **(a)** according to the presence or absence of 1 or 2 HLA-DR-SE alleles or HLA-DRB1*14:02 with any HLA-DR-SE allele, and **(b)** according to presence or absence of a single HLA-DR-SE or HLA-DRB1*14:02 allele, as shown. Each column represents one patient sample.

Figure 2. Accommodation of arginine and citrulline residues by HLA-DRB1*01:01, DRB1*04:01 and DRB1*14:02. (a) The peptide binding groove of a HLA-DR molecule is shown in cartoon with polymorphic residues shown as sticks corresponding to the residues present in HLA-DRB1*14:02, which is associated with RA among the INA. Schematic representation of the differences in pockets between HLA-DRB1*14:02 (red font), *04:01 (black font) and *01:01 (blue font). (**b**) Competitive binding of a biotin-labelled $HA_{305-319}$ peptide with an unlabelled $HA_{305-319}$ peptide or $HA_{305-319}$-variants with citrulline or arginine residues in P1, P4, P6, P7 and P9 to HLA-DRB1*01:01 , DRB1*04:01 and DRB1*14:02. ND = Non-detectable binding affinity. Pooled binding data from at least 3 experiments are shown and error bars depict the variation between experiments. (**c**) Competitive binding of a biotin-labeled $HA_{305-319}$ peptide with unlabeled $vimentin_{59-71}$ and $vimetin\text{-}64Cit_{59-71}$ to HLA-DRB1*01:01, *04:01 and *14:02.

Figure 3. Crystal structure of HLA-DRB1*1402 in complex with $vimentin_{59-71}$, $vimentin\text{-}64Cit_{59-71}$ and $fibrinogen\beta\ 74Cit_{69-81}$

The α- and β-chains of (a) the HLA-DRB1*1402 in complex with vimentin$_{59-71}$ are shown in cartoon representation and coloured in light green and light blue respectively, while peptide is displayed as sticks. Side view of (b) HLA-DRB1*1402-vimentin$_{59-71}$, (c) HLA-DRB1*1402-vimentin-64Cit$_{59-71}$ and (d) HLA-DRB1*1402-fibrinogenβ74Cit$_{69-81}$. The carbons are coloured deep salmon, light orange and teal for vimentin$_{59-71}$, vimentin-64Cit$_{59-71}$ and fibrinogenβ 74Cit$_{69-81}$, respectively, nitrogens are coloured in blue and oxygens are coloured in red. The β-chain is transparent to help visualize the peptide. The unbiased 2Fo-Fc electron density map of the peptides is shown in blue and contoured to 1 σ. (e) Superposition of the three peptides bound to HLA-DRB1*1402. The P4 pocket of HLA-DRB1*1402 bound to (f) vimentin$_{59-71}$, (g) vimentin-64Cit$_{59-71}$ and (h) fibrinogen β 74Cit$_{69-81}$. The P4-Arg in the vimentin$_{59-71}$ peptide is buried in the P4 pocket, The P4-Cit of the vimentin-64Cit$_{59-71}$ and fibrinogen β 74Cit$_{69-81}$ peptide adopts an upright conformation

Figure 4. Presentation of vimentin$_{59-71}$ and vimentin-64Cit$_{59-71}$ self-antigens in context of HLA-DRB1*14:02 to CD4$^+$ T cells in individuals with and at high risk of ACPA$^+$ RA.

(**a-d**) PBMC from HLA-DRB1*14:02$^+$ RA patients W1:1-10 and HLA-DRB1*14:02$^+$ FDR W1:1-10 were stained with PE-labelled HLA-DRB1*1402-vimentin64Cit$_{59-71}$ or HLA-DRB1*14:02-vimentin$_{59-71}$ tetramer, CD4-APC, CD25-PE/Cy7, and CD127-BV421. Live CD4+ FITC-lineage-negative tetramer+ T cells were gated based on an FMO sample stained with unlabelled primary and conjugated secondary antibodies. The number calculated relative to the CD4$^+$ T cell count, (**a**) and mean fluorescence intensity (MFI) (**b**) of tetramer$^+$ cells within the total CD4$^+$ population is shown for RA patients and FDR; (**c**) the proportion of CD4$^+$CD25$^+$CD127$^+$ Teff and CD4$^+$CD25$^+$CD127$^-$ Treg within vimentin64Cit$_{59-71}$-reactive and vimentin$_{59-71}$-reactive CD4$^+$ T cell gates and the total CD4+ gate is shown for pooled RA patients and FDR. (**d**) The numbers of vimentin64Cit$_{59-71}$-reactive and vimentin$_{59-71}$-reactive CD4$^+$ T cells were correlated in pooled RA patients and FDR (R^2 0.74, $p<0.0001$). (**e**) The

Teff/Treg ratio of vimentin64Cit$_{59-71}$ and vimentin$_{59-71}$-reactive CD4$^+$ T cells is plotted relative to total CD4$^+$ T cell ratio in pooled RA patients and FDR; (**f**) CD45RO$^+$CD28$^+$, (**g**) CD45RO$^+$CD69$^+$ and CD45RO$^+$CD69$^+$ NKG2D$^+$ vimentin$_{59-71}$-reactive CD4$^+$, vimentin64Cit$_{59-71}$-reactive CD4$^+$ and total CD4$^+$ T cells are plotted in pooled RA patients W2:1-3 and FDR W2:1-3. (**h**) Frequencies of V-J pairing for TCRα and TCRβ among vimentin64Cit$_{59-71}$-specific and vimentin$_{59-71}$-specific CD4$^+$ T cells from HLA-DRB1*14:02$^+$ RA patients (n=5) and FDR (n=5), and tetramer-negative CD3$^+$ T cells sorted from DRB1*14:02$^+$ RA patients (n=3). The width of the bands is proportional to the frequency of TCR sequences with a particular V-J pairing. Details of productive TCRα and TCRβ sequences in Supplementary Table 4 and Table 2. The figures were generated using the Circos online Table Viewer software (http://mkweb.bcgsc.ca/tableviewer/). (**i**) 10^6 P2F3 SKW3 cells were stimulated with 5 ng/mL unlabelled HLA-DRB1*14:02-vimentin$_{59-71}$ or HLA-DRB1*14:02-vimentin-64Cit$_{59-71}$ tetramer for 4 hours at 37°C. Cells were fixed and permeabilised, then stained with PerCP/ Cy5.5-ERK1/2 and PB-CD3. Live CD3$^+$ cells expressing the GFP marker gene were gated. Need to indicate how many times this experiment was done.

Tables

Table 1. Association of HLA-DRB1*14:02 with all RA and seropositive RA in INA RA patients and controls.

Patients and controls were stratified according to the presence of SE. SE-positive individuals were further stratified as shown. Other SE-alleles included DRB1*01:01, *01:02, *04:01, *04:04, *04:05, *04:08, *04:10, *04:13, and *10:01. HC: healthy controls.

	HC n (%)	**All RA** n (%)	**OR** (CI)	***P***	**Seropositive RA,** n (%)	**OR** (CI)	***P***
SE^-	106 (30)	51 (15)	REF		32 (15)	REF	
$14:02^+$/ other SE^-	64 (18)	80 (23)	2.60 (1.63-4.15)	0.0001	46 (21)	2.38 (1.38-4.12)	0.0019
$14:02^-$/ other SE^+	147 (42)	178 (52)	2.52 (1.69-3.75)	<0.0001	117 (54)	2.64 (1.66-4.19)	<0.0001
$14:02^+$/ other SE^+	35 (10)	35 (10)	2.08 (1.17-3.70)	0.0127	23 (11)	2.18 (1.13-4.20)	0.02
Any SE^+	246 (70)	293 (85)	2.48 (1.70-3.60)	<0.0001	186 (85)	2.46 (1.58-3.81)	0.0001

Table 2. Repeated TCR TRAV, TRBV and TRAV/TRBV clonotypes used by HLA-DRB1*14:02-restricted vimentin$_{59-71}$ or vimentin64Cit$_{59-71}$-reactive CD4$^+$ T cells.

TCR repertoire analysis was undertaken in RA patients W1:1-5 and FDR W1:1-5. Productive single TRAV and TRBV clonotypes detected from 2 RA patients and 3 FDR are shown. Frequency reflects the frequency of the repeated TRAV or TRBV clonotype divided by the total number of tetramer$^+$ cells with productive TRAV or TRBV sequence, for each individual. *^ nucleotide sequences encoding each of the public CDR3β amino acid sequences, which require a minimal number of N or P additions to be produced. Nucleotides attributed by the germline Vβ, Dβ and Jβ genes are shown in blue, red and green respectively. N-additions are in black and P-additions in purple text. The nucleotides at the D-J junction encoding the same amino acid are underlined in each case.

Subject	**Tetramer**	**TRAV**	**CDR3α**	**TRAJ**	**Frequency no./total, (%)**	***HLA-DRB1***
RA W1:1	Cit-vimentin	13-2	SQPGTAL	15	2/17 (11.8%)	14:02, 14:02
RA W1:2	Vimentin	26-1	SGAGSYQL	28	5/13 (38%)	04:04, 14:02
Subject	**Tetramer**	**TRBV**	**CDR3β**	**TRBJ**	**Frequency* (%)**	
RA W1:1	Cit-vimentin	2	SEAADNEQ	2-1	2/14 (14.2%)	14:02, 14:02
RA W1:2	Vimentin	10-3	GGTRTESSYEQ	2-7	2/5 (40%)	04:04, 14:02
*FDR W1:3	Cit-vimentin	30	SIGAGNQPQ	1-5	1/19 (5.2%)	04:04, 14:02
*FDR W1:3	Vimentin	30	SIGAGNQPQ	1-5	3/7 (42.8%)	
^FDR W1:5	Cit-vimentin	30	SVGAGNQPQ	1-5	2/2 (100%)	13:02, 14:02
^FDR W1:5	Vimentin	30	SVGAGNQPQ	1-5	2/6 (33%)	
Subject	**Tetramer**	**TRAV/ TRBV**	**CDR3a/CDR3β**	**TRAJ/ TRBJ**	**Frequency* (%)**	
RA W1:1	Cit-vimentin	13-2/2	SQPGTAL/ SEAADNEQ	15/ 2-1	2/12 (16.6%)	14:02, 14:02

Subject	TRBV									
*FDR W1:3	30*01	S	I	G	A	G	N	Q	P	Q
		agt	atc	ggg	gcg	ggc	aat	cag	ccc	cag
^FDR W1:5	30*01	S	V	G	A	G	N	Q	P	Q
		agt	gtg	ggg	gca	ggc	aat	cag	ccc	cag

Figure 1

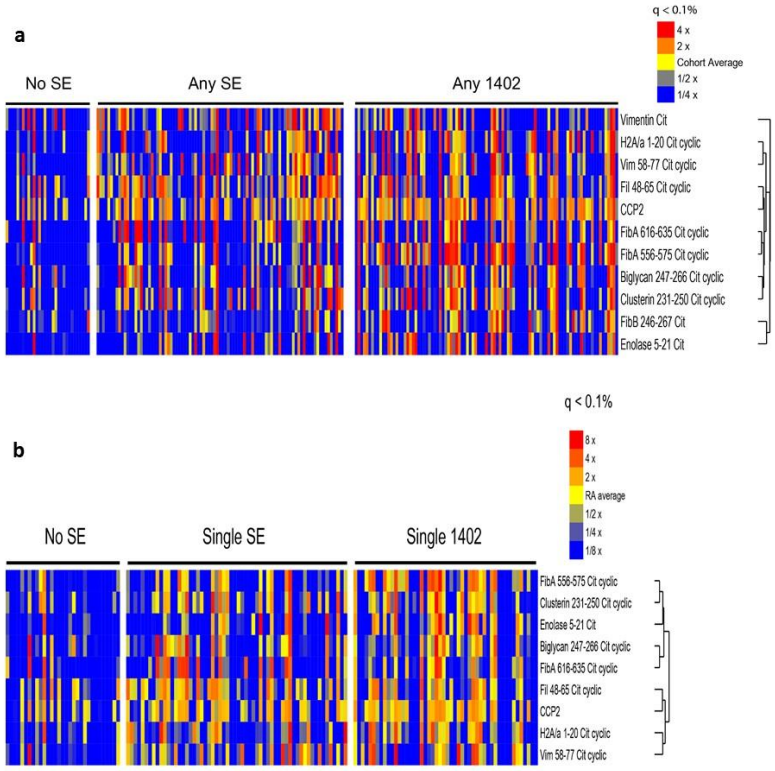
a
q < 0.1%
4 x
2 x
Cohort Average
1/2 x
1/4 x
No SE
Any SE
Any 1402
Vimentin Cit
H2A/a 1-20 Cit cyclic
Vim 58-77 Cit cyclic
Fil 48-65 Cit cyclic
CCP2
FibA 616-635 Cit cyclic
FibA 556-575 Cit cyclic
Biglycan 247-266 Cit cyclic
Clusterin 231-250 Cit cyclic
FibB 246-267 Cit
Enolase 5-21 Cit
b
q < 0.1%
8 x
4 x
2 x
RA average
1/2 x
1/4 x
1/8 x
No SE
Single SE
Single 1402
FibA 556-575 Cit cyclic
Clusterin 231-250 Cit cyclic
Enolase 5-21 Cit
Biglycan 247-266 Cit cyclic
FibA 616-635 Cit cyclic
Fil 48-65 Cit cyclic
CCP2
H2A/a 1-20 Cit cyclic
Vim 58-77 Cit cyclic

Figure 2

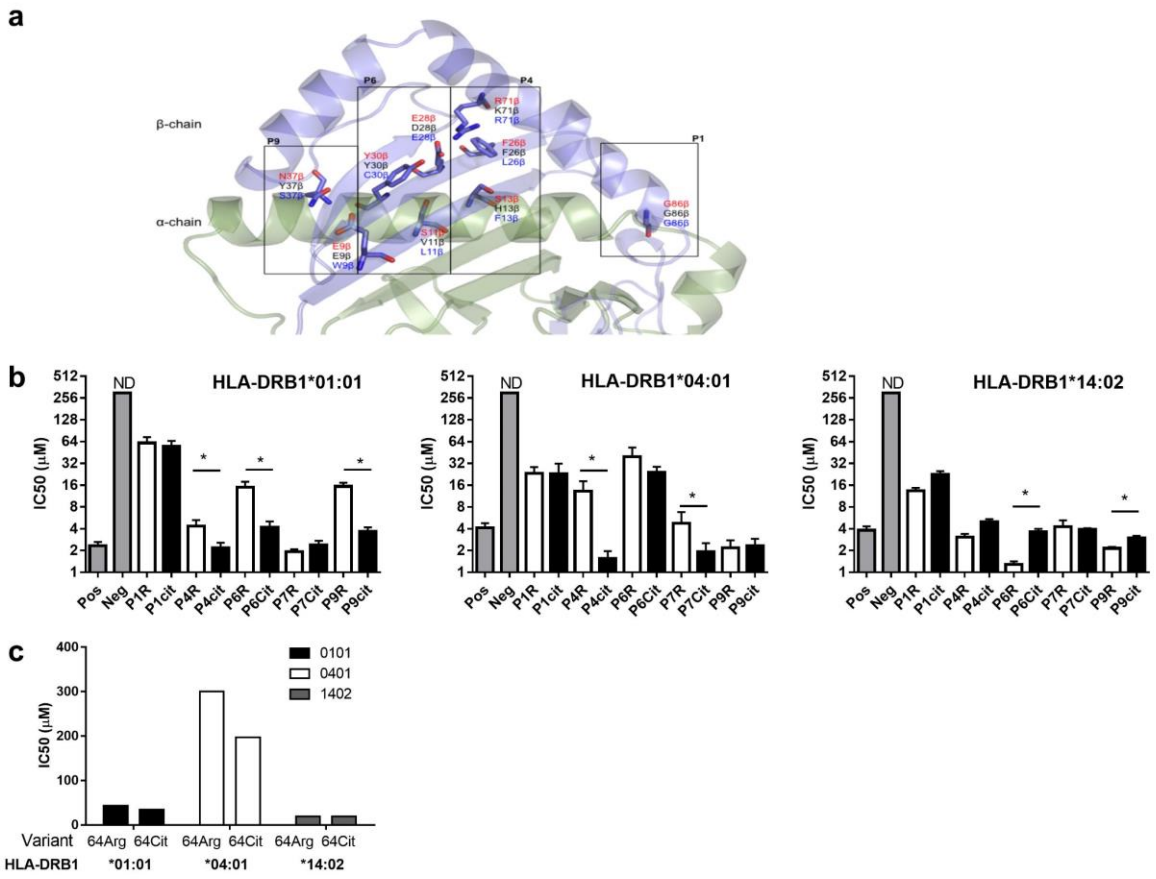
a
β-chain
α-chain
P6
P4
P9
P1
b
HLA-DRB1*01:01
HLA-DRB1*04:01
HLA-DRB1*14:02
IC50 (μM)
ND
Pos
Neg
P1R
P1cit
P4R
P4cit
P6R
P6Cit
P7R
P7Cit
P9R
P9cit
c
0101
0401
1402
Variant
64Arg
64Cit
HLA-DRB1
*01:01
*04:01
*14:02

Figure 3

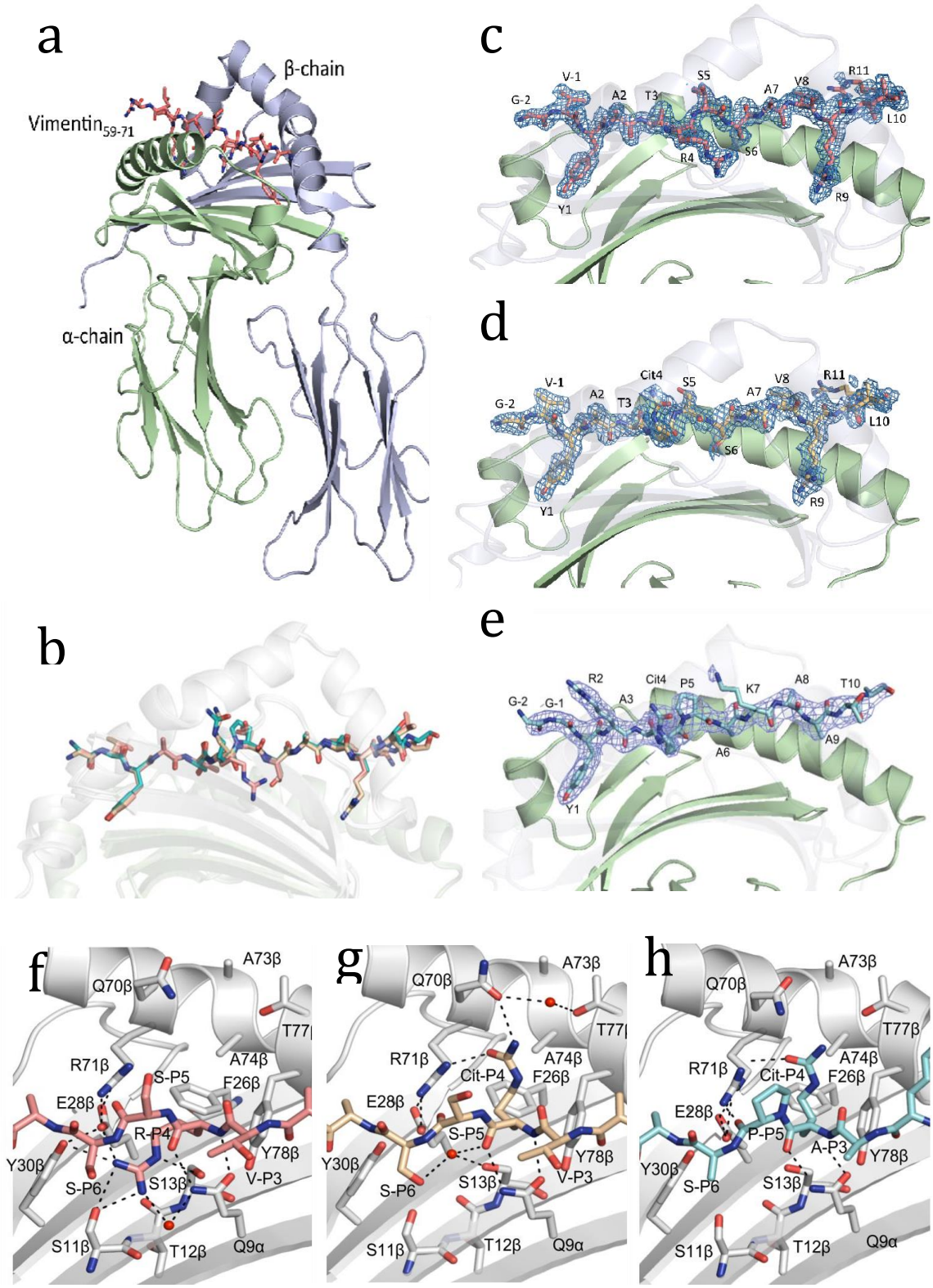
a
β-chain
Vimentin59-71
α-chain
c
V-1
G-2
A2
T3
S5
A7
V8
R11
L10
R4
S6
R9
Y1
d
V-1
Cit4
S5
G-2
A2
T3
A7
V8
R11
L10
S6
R9
Y1
b
e
R2
Cit4
P5
K7
A8
T10
G-2
G-1
A3
A9
A6
Y1
f
A73β
Q70β
T77β
R71β
A74β
S-P5
F26β
E28β
R-P4
Y78β
Y30β
S-P6
S13β
V-P3
S11β
T12β
Q9α
g
A73β
Q70β
T77β
R71β
A74β
Cit-P4
F26β
E28β
S-P5
Y78β
Y30β
S-P6
S13β
V-P3
S11β
T12β
Q9α
h
A73β
Q70β
T77β
R71β
A74β
Cit-P4
F26β
E28β
P-P5
A-P3
Y78β
Y30β
S-P6
S13β
S11β
T12β
Q9α

Figure 4

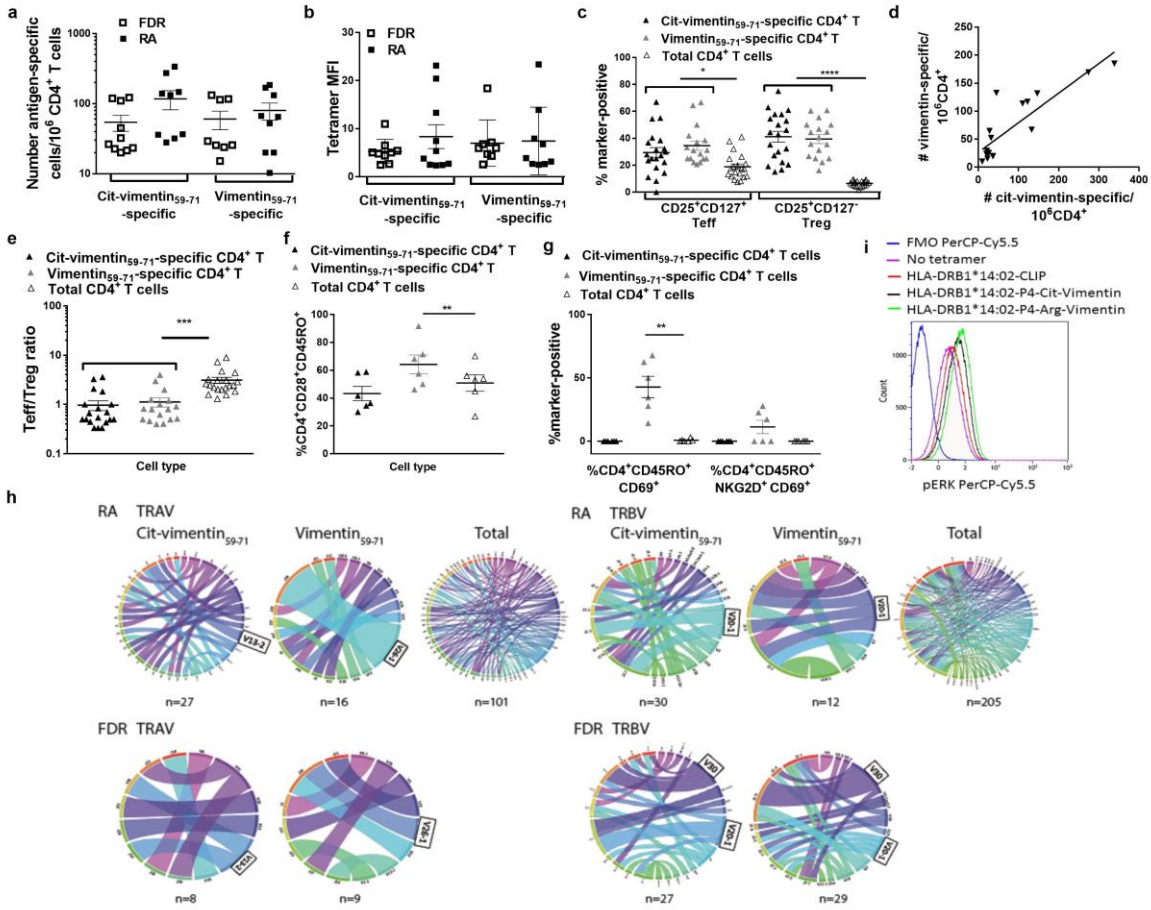
a
FDR
RA
Number antigen-specific cells/10^6 CD4+ T cells
Cit-vimentin59-71 -specific
Vimentin59-71 -specific
b
FDR
RA
Tetramer MFI
Cit-vimentin59-71 -specific
Vimentin59-71 -specific
c
Cit-vimentin59-71-specific CD4+ T
Vimentin59-71-specific CD4+ T
Total CD4+ T cells
% marker-positive
CD25+CD127+ Teff
CD25+CD127- Treg
d
vimentin-specific/ 10^6CD4+
cit-vimentin-specific/ 10^6CD4+
e
Cit-vimentin59-71-specific CD4+ T
Vimentin59-71-specific CD4+ T
Total CD4+ T cells
Teff/Treg ratio
Cell type
f
Cit-vimentin59-71-specific CD4+ T
Vimentin59-71-specific CD4+ T
Total CD4+ T cells
%CD4+CD28+CD45RO+
Cell type
g
Cit-vimentin59-71-specific CD4+ T cells
Vimentin59-71-specific CD4+ T cells
Total CD4+ T cells
%marker-positive
%CD4+CD45RO+ CD69+
%CD4+CD45RO+ NKG2D+ CD69+
i
FMO PerCP-Cy5.5
No tetramer
HLA-DRB1*14:02-CLIP
HLA-DRB1*14:02-P4-Cit-Vimentin
HLA-DRB1*14:02-P4-Arg-Vimentin
Count
pERK PerCP-Cy5.5
h
RA TRAV
Cit-vimentin59-71
Vimentin59-71
Total
n=27
n=16
n=101
RA TRBV
Cit-vimentin59-71
Vimentin59-71
Total
n=30
n=12
n=205
FDR TRAV
n=8
n=9
FDR TRBV
n=27
n=29